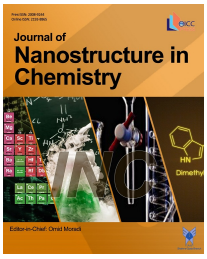

Volume 15, Issue 5, 152517 (1-11)

Journal of Nanostructure in Chemistry (JNSC)

https://doi.org/10.57647/jnsc.2025.1505.17

Cr_2C MXene Modification of an Electrochemical Platform Allows for Highly Selective and Sensitive Detection of PSMA, a Prostate Cancer Biomarker

Yi Xu[1], Lijun Wan[2], Najmeh Zare[1,4,*], Si-Wei Wang[3,*], Zhangming Lei[2,*]

[1]*Department of Urology, Department of Science & Technology, BioSensorMed Research Group, The Quzhou Affiliated Hospital of Wenzhou Medical University, Quzhou People's Hospital, Quzhou, Zhejiang 324000, PR China.*
[2]*Department of Urology, The Quzhou Affiliated Hospital of Wenzhou Medical University, Quzhou People's Hospital, Quzhou, Zhejiang 324000, PR China.*
[3]*Department of Pharmacy, BioSensorMed Research Group, The Quzhou Affiliated Hospital of Wenzhou Medical University, Quzhou People's Hospital.*
[4]*Department of Chemical Engineering, Quchan University of Technology, Quchan, Iran.*

*Corresponding authors: najmeh.zare.1997@gmail.com, wsw_1972@wmu.edu.cn, zhangming.lei@hotmail.com

Original Research

Received:
1 August 2025
Revised:
15 September 2025
Accepted:
28 September 2025
Published online:
2 October 2025

Abstract:

Prostate cancer represents a significant global health challenge, being the most common malignancy among men and a leading cause of cancer-related mortality. The pressing demand for novel diagnostic approaches is evident. In this work, we introduce an advanced biosensor aimed at facilitating rapid and accurate detection of prostate cancer, specifically through the quantification of prostate-specific membrane antigen (PSMA). The biosensor is constructed by modifying a screen-printed carbon electrode (SPCE) with gold nanoparticles (AuNPs) and a Cr_2C MXene nano layer catalyst, combined with a pb^{2+}-binding aptamer (AP) (SPCE/Cr_2C MXene/AuNPs/Pb^{2+}-AP). This novel design demonstrates exceptional specificity and affinity for PSMA, enabling highly sensitive quantification across a linear dynamic range of 1.0 to 850 pg/mL. Characterization techniques, including TEM, SEM, EDS, AFM, XPS, BET analysis, and XRD, confirm the success synthesis of the Cr_2C MXene layer, which serves as an effective support for integrating the biological recognition element. Given the high mortality associated with prostate cancer and the critical need for early detection, this biosensor offers a promising tool for clinical diagnostics, capable of selectively identifying PSMA in the presence of other biomarkers. The implications of this work extend beyond the laboratory, potentially transforming prostate cancer management and improving patient outcomes.

Keywords: Electrochemical biosensor; PSMA; Cr_2C MXene; Biosensor; Single-stranded DNA

Cite this article: Xu, Y., Wan, L., Zare, N., Wang, S.-W., Lei, Zh. Cr_2C MXene Modification of an Electrochemical Platform Allows for Highly Selective and Sensitive Detection of PSMA, a Prostate Cancer Biomarker. *J Nanostruct Chem* **15**(5), 152517 (2025).

1. Introduction

Outlined by World Health Organization (WHO) in 2019, cancer has been declared to be one of the most concerning global health issues affecting almost 183 nations as its precedent increases year after year. Described as the first or second leading cause of mortality among individuals under seventy suffering from the illness across 112 countries, it is clear just how significant a threat it poses to the economy. Cancer is dangerous not only because it can be fatal, but also because it hinders improvements in life expectancy, leading to additional challenges for society [1]. In an additional 23 countries, it ranks third or fourth which highlights the global demand for improving research, prevention, and treatment efforts [2, 3]. Prostate cancer is the second most prevalent cancer diagnosed in men worldwide, underscoring its importance as a public health concern [4]. The high incidence of prostate cancer emphasizes the urgent need for improved screening and early detection methods [5]. Biological markers (biomarkers) are measurable cellular or molecular indicators of biological processes, disease states,

or treatment responses, assisting in disease prediction, diagnosis, and evaluation [6–9]. While they are valuable for drug development and research, biomarkers do not always align with a patient's clinical experience [10–12]. There are a wide variety of prostate cancer biomarkers such as PSMA, PCA3 and so on. PSMA is a unique cell-surface protein that shows a significant over-expression on prostate cancer cells, especially in advanced stage prostate carcinomas with low expression in normal human tissue. Its elevated levels in prostate cancer tissues can be used to detect the disease more effectively and monitor treatment responses [13]. Traditional PSMA detection methods, such as immunohistochemistry and PET scanning, are likely to have significant limitations, including reduced sensitivity, reliance on technical expertise, and the need for invasive tissue biopsies. They can yield false negatives, will need special equipment and experienced personnel, and may not be readily available in all medical facilities [14, 15]. Additionally, the multi-step nature of these procedures is often time-consuming, and their outcomes can vary based on individual interpretation. It is evident that biomarker monitoring and therapeutic interventions, which are tailored by clinicians, can improve patient care and outcomes. In this context, biosensors offer a rapid and sensitive detection strategy for quick analysis. The devices convert bio-signals to measurable outputs, facilitating ease in tumor biomarkers detection and allowing timely and optimized treatment protocols. Electrochemical sensing provides highly sensitive and selective detecting capability that finds special utility in environmental monitoring and medical diagnostics [16–19]. MXene is a term for a class of two-dimensional (2D) materials known as MXene that are transition metal carbides, nitrides, and carbonitrides having the general formula Mn+1XnTX [20]. They are prepared from layered MAX phases precursors containing a transition metal 'M', an 'A' group element, and carbon or nitrogen 'X' [21–23]. The process of synthesis is through exfoliation of the 'A' layers to produce MXene sheets with potentially tunable surface terminations marked by TX (for example, -F, -O, -OH) [24, 25]. MXene also have a wide range of highly versatile applications in various areas, more in the biomedical field, due to their excellent properties [26–29]. Their hydrophilic, antimicrobial behavior and bio compatibility make them compatible with skin repair applications. Cr_2CTx MXene, in particular, has strong antibacterial activities against gram-negative and gram-positive bacteria, which make them increasingly useful in wound healing. They also possess anti-fungal activity to assist in wound healing. They are also highly efficient in photothermal conversion, making them good for use in solar energy. MXene are fit for sensor and electronic device use and, through hydrophilic nature, can be easily functionalized, making them more useful in composite materials [30–33]. Apart from that, MXene are also playing an important role in applications of electro-catalysis and energy storage, particularly as supports for single-atom catalysts (SACs) that improve catalytic efficiency in significant reactions like hydrogen evolution. Their distinct properties enhance efficiency in energy storage systems. MXene-based SACs are also employed in various sensing technologies, capitalizing on their attributes to improve detection capabilities [34, 35]. Notably, MXene show great promise in electrochemical sensors, where their high conductivity and advantageous surface characteristics can greatly enhance sensitivity and selectivity, makes them suitable for detecting biochemical substances in medical diagnostics and environmental monitoring. This work introduces an advanced electrochemical sensor based on MXene, with the incorporation of gold nanoparticles (AuNPs). The addition of AuNPs significantly improves the sensitivity of the sensor and offers a platform for prostate-specific membrane antigen binding. This new sensor is targeted at achieving high sensitivity and specificity towards the detection of PSMA, hence offering a potential strategy for the further enhancement of the diagnosis and treatment of prostate cancer (PCa). The focus of the study was on developing a label-free electrochemical sensing device utilizing aptamers, featuring Cr_2C MXene nanosheets combined with AuNPs to enhance the detection capabilities for the PSMA biomarker. A thiol-functionalized PSMA aptamer preloaded with Pb^{2+} ions was anchored onto the electrode surface to serve as the recognition element. This configuration enables the development of a non-invasive electrochemical platform for PSMA detection, which is crucial for monitoring prostate cancer in patients. To identify the Pb^{2+} ions associated with the aptamer as a signaling indicator, square wave anodic stripping voltammetry (SWASV) was employed, providing a highly sensitive measurement technique. Signal fluctuations were observed upon the release of Pb^{2+} ions from the surface of Cr_2C MXene/AuNPs when PSMA and aptamer interacted. The choice of Pb^{2+} as the signaling ion in the biosensor designed for medical diagnostics, particularly for detecting PSMA, is primarily due to its strong electrochemical properties, which enhance the sensor's sensitivity and specificity. Pb^{2+} ions can effectively bind to the aptamer, providing a measurable signal change upon interaction with the target biomarker, PSMA. This interaction allows for precise quantification of PSMA concentrations, which is crucial for early detection and monitoring of prostate cancer. On the other hand, the presence of gold nanoparticles in the fabrication of aptamer biosensors enhances conductivity and sensitivity while facilitating stable binding through the interaction between the nanoparticles and the thiolic groups at the ends of the aptamer structure. The innovative design not only enhances detection sensitivity but also allows for monitoring of PSMA concentration in real samples, which is a prerequisite for early intervention during prostate cancer treatment. The SPCE/Cr_2C MXene/AuNPs/Pb^{2+}-AP offers many advantages compared to previously suggested biosensors for PSMA detection, such as a better dynamic range due to the high surface area of the biosensor from the presence of Cr_2C MXene, and a good limit of detection due to the synergistic effect of Cr_2C MXene and gold nanoparticles in the modification of the biosensor. This suggests that this biosensor is a powerful tool for the diagnosis of PSMA.

2. Experimental part

2.1 Components and reactants

Chromium Aluminum Carbide (Cr_2AlC; 99%) was procured from Laizhou Kai Kai Ceramic Materials Co., Ltd. in Shandong, China. Tris (hydroxymethyl) aminomethane (Tris), 6-Mercaptohexanol (MCH), Lithium fluoride (LiF; 99.9%), hydrochloric acid (HCl; 35%), Tris (2-carboxyethyl) phosphine hydrochloride (TCEP), chloroauric acid ($HAuCl_4$; 99.99%), potassium chloride (KCl; 99.99%) and lead(II) nitrate ($Pb(NO_3)_2$; 99.0%) were sourced from Adamas (Shanghai Titan Scientific Co, Ltd., located in China). All chemicals employed in this study were of analytical grade and used without further purification. Each experiment was performed in quadruplicate to ensure reproducible and reliable responses. The DNA aptamer bearing a thiol modification was procured from Sangon Biotech (Shanghai, China) with the sequence listed below:
5′-SHC6-
GGGAGGACGAUGCGGAUCAGCCAUGUUUACGUCA
CUCCUUGUCAAUCCUCAUCGGC-3′.

2.2 Cr_2C-MXene Synthesis

The synthesis of MXene refers to this reports [36]. To prepare the etching medium, 4 mL of hydrochloric acid solution (2 M) was employed to dissolve 0.4 g of lithium fluoride, and the mixture was stirred for approximately 5 min. Subsequently, 0.2 g of Cr_2AlC precursor powder was added slowly into the prepared solution and maintained under continuous stirring at ambient conditions for 48 h, enabling selective removal of aluminum layers. After etching, the dispersion was subjected to centrifugation at 4000 rpm for 10 min, followed by repeated washing with deionized water until the pH of the supernatant exceeded 5. To achieve efficient exfoliation of Cr_2C nanosheets, the resulting suspension was further treated by vortex agitation for 30 min. A subsequent centrifugation step (10 min) was carried out to separate the supernatant, which was dried in an oven at 60 °C to yield Cr_2C MXene powder.

2.3 Fabrication of SPCE/Cr_2C MXene/AuNPs/Pb^{2+}-AP

Electrochemical measurement was performed in a 10 mM Tris-HCl buffer at pH 7.4 and room temperature). A 5.0 µL Cr_2C-MXene suspension (0.5 mg/mL) was cast onto the SPCE surface and dried under infrared light. The SPCE/Cr_2C MXene was then immersed in a 0.01 M $HAuCl_4$ solution with 0.1 M KCl, where electrodeposition was performed at −0.3 V for 1 minute, followed by air drying. Finally, a Pb^{2+}-aptamer solution was added onto the SPCE/Cr_2C MXene/AuNPs surface and incubated for 12 hours at 4 °C. The electrode surface was first washed with Tris-HCl buffer to eliminate loosely attached species, followed by modification with 1.0 mM MCH for 1 h. Afterward, the surface was rinsed to remove any excess molecules and subsequently incubated with PSMA solution. The prepared interface was then subjected to electrochemical analysis using SWASV, as illustrated in scheme 1.

3. Results and discussions

3.1 Analysis of MXene catalyst

The morphology and microstructure of MXene were analyzed using SEM and TEM techniques, as depicted in

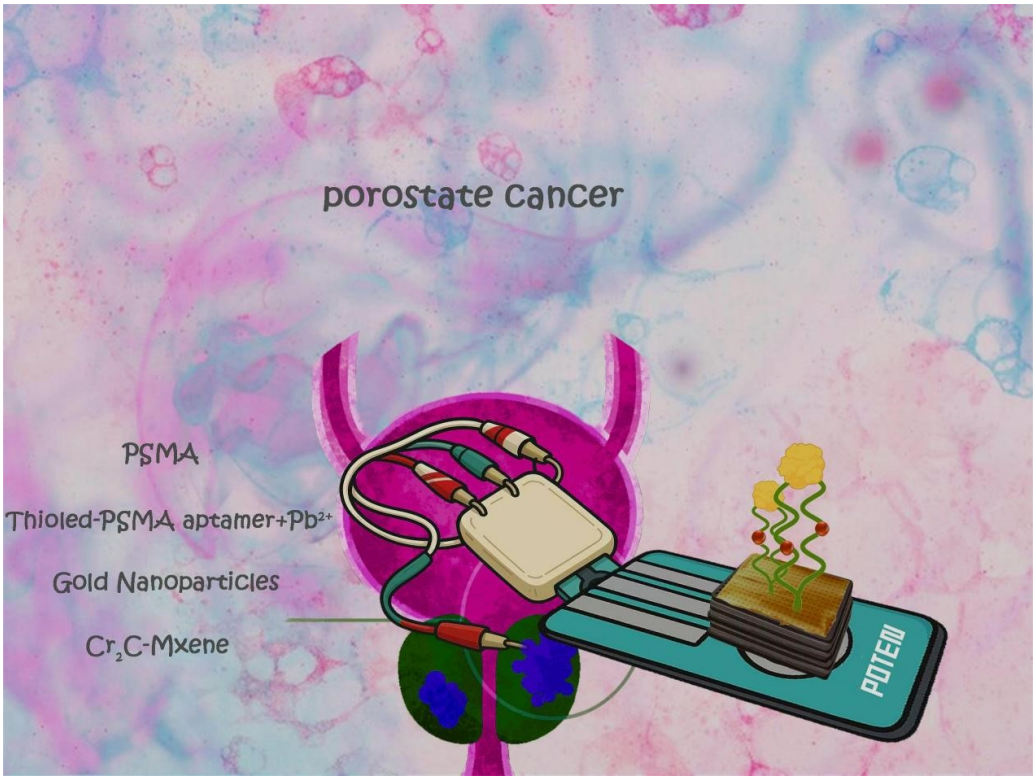

Scheme 1. A diagram depicting the steps involved in creating the aptamer biosensor design utilized for PSMA detection.

figure1.

After treating the precursor with LiF and HCl to remove the aluminum layer, a clear two-dimensional multilayered structure was observed, confirming the successful synthesis of MXene Fig. 1 (a-c). The EDS characterization results in Fig. 1 (d) further demonstrate that the synthesized MXene composite comprises two elements C, O, Cl, and Cr validating its successful creation. Moreover, the high-resolution TEM image shown in Fig. 1 (e-g) provides insights into the lattice plane spacing of the MXene material. This detailed analysis illustrates the effective removal of impurities and the formation of the desired MXene structure with distinct layered characteristics.

Atomic force microscopy was used to investigate the Cr_2C MXene structure, and the resulting image is presented in Fig. 2 (a). Microscopic examination reveals distinct sheet-like layers, which provide strong evidence that the aluminum component was successfully eliminated during etching, leading to the formation of Cr_2C MXene with the anticipated few-layer thickness.

BET analysis is a standard technique used to measure the surface area of solids. This technique is especially beneficial for investigating the surface characteristics of various solids, providing researchers and scientists with valuable insights into the materials' structural properties and behaviors [37, 38]. Fig. 2 (b) demonstrates the BET method analysis indicates that the Cr_2C sample has a relatively low specific surface area of approximately 1.88 m^2/g. Besides, the sum pore volume is around 0.10 mL/g as a result of mostly macro-pores. This result also emerges from the plots for pore size distribution calculated from BJH and NLDFT both of which indicate an average pore diameter between 76 and 101 nm consistent with a predominantly macro-porous nature. The observed low BET surface area is likely due to insufficient delamination and exfoliation steps, which may restrict the sensor's ability to achieve optimal sensitivity by

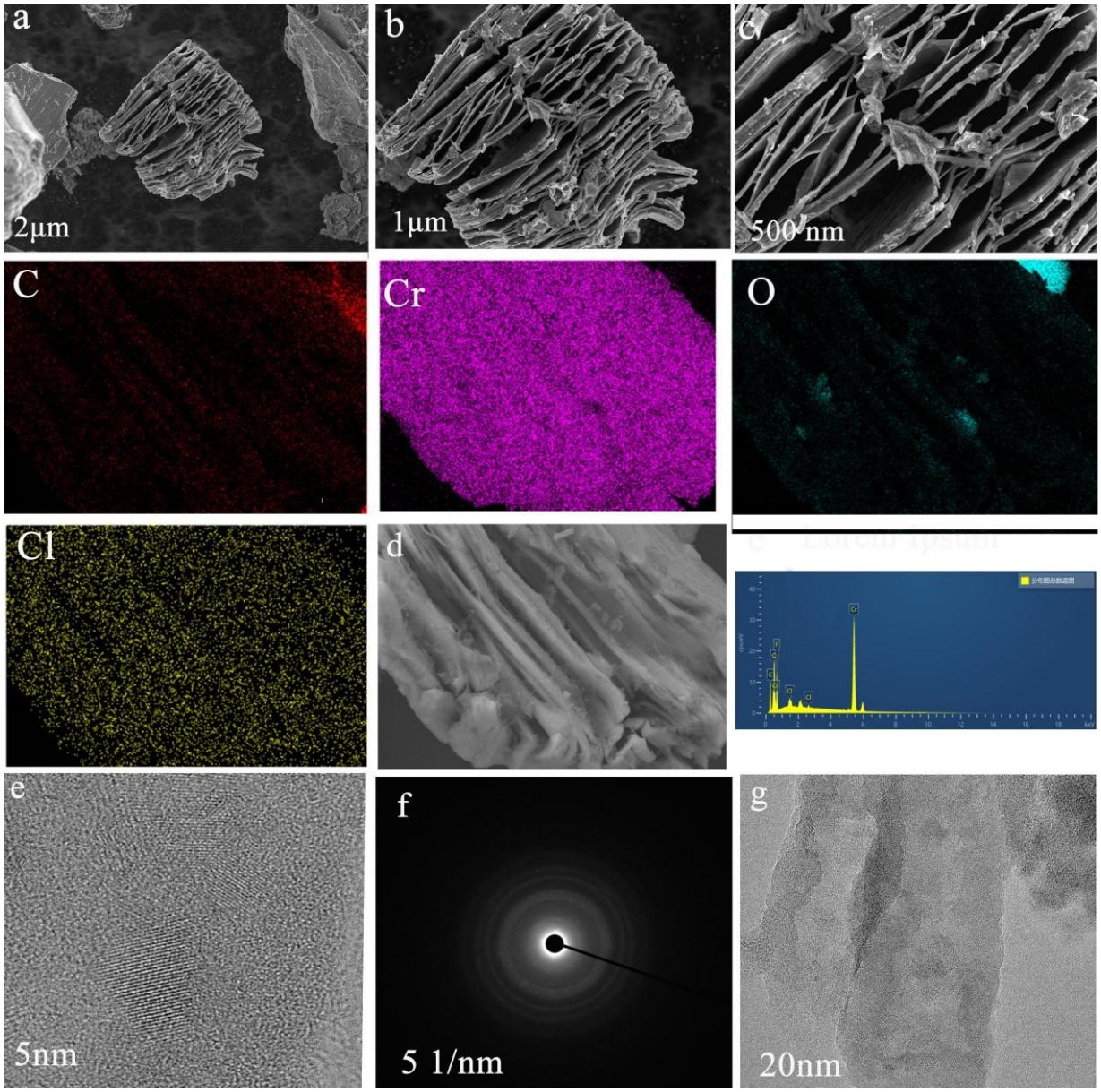

Figure 1. SEM analysis of MXene (a-c), along with elemental mapping and EDS spectrum (d) and TEM image of Multi-layer MXene (e-g).

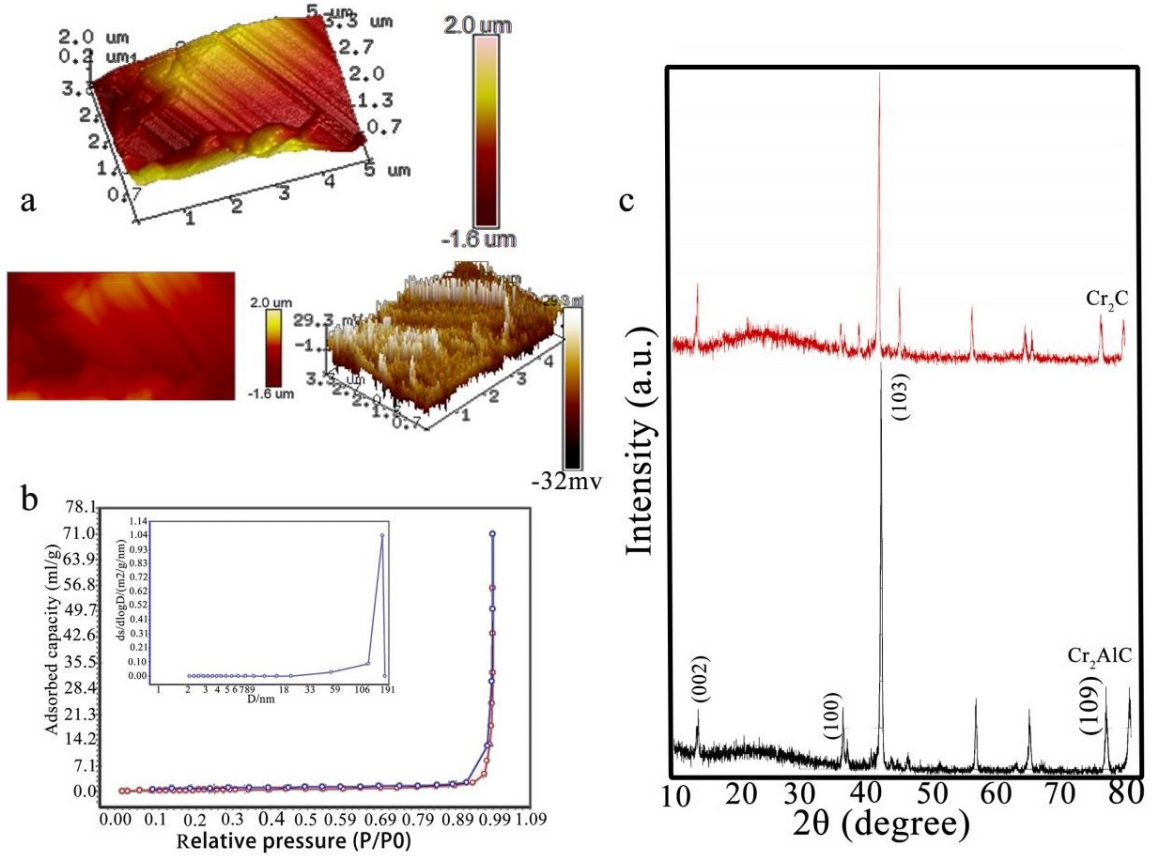

Figure 2. AFM image of Cr_2C MXene (a), nitrogen adsorption-desorption isotherms (BET) of Cr_2C MXene (b), and XRD patterns of Cr_2C MXene and the Cr_2AlC MAX phase (c).

reducing the available active sites for biomolecule binding. Therefore, modifications to the synthesis process, such as incorporating additional delamination or exfoliation techniques like sonication, are recommended to enhance the active surface area and improve the sensor's performance.

XRD pattern of synthesized MAX phase Cr_2AlC is shown in Fig. 2 (c), consisting of sharp peaks that indicate successful synthesis. The peaks at $2\theta = 14.1°$, 36.4,°42.4°, and 77.3° correspond to the (002), (100) and (109) planes, reflecting the hexagonal structure of the prepared MAX phase [39, 40]. Following synthesize, the characteristic reflections of the MAX phase showed a marked decrease in intensity accompanied by a shift to higher diffraction angles, indicating that the synthesis was successfully accomplished and aligning with reported XRD patterns of Cr_2C MXene and the utilized MAX phase [41].

Figure3 has been utilized to compare the surface chemical composition and states of XPS-synthesized Cr_2CT_x MXene. The survey spectrum as indicated by Fig. 3 (a) confirmed the presence of chromium, carbon, oxygen, fluorine, and chlorine and showed successful etching of the MAX phase. Figure3 (b) shows High-resolution C_{1s} analysis showed peaks at 284.43 eV (C–C), 285.96 eV (C–O), 288.02 eV (C=O), and 291.82 eV (C–F) and also a peak at 282.04 eV for C–Cr bonds, which confirms carbide structure retention. The O_{1s} spectrum showed peaks at 529.60 eV and 531.17 eV, corresponding to metal–oxygen bonds and C–O functional groups, respectively [42, 43]. The Cr_{2p} spectrum in Fig. 3 (d) suggested that chromium primarily exists in the +3 oxidation state. The quantification of surface terminations indicates specific ratios of –O, –OH, and –F groups, impacting the surface chemistry. These varied terminations and stable Cr–C bonding suggest that Cr_2CT_x MXene is promising for gas sensing applications, particularly for NO_2 detection, with its partial oxidation potentially affecting sensitivity. Specifically, oxidation can create additional active sites for gas adsorption, enhancing the sensor's response. However, it may also lead to changes in electronic properties, which could either improve or hinder sensitivity depending on the context. Moreover, the high electrical conductivity of MXene enhances their sensing capabilities. Keep in mind that XPS spectra of MXene are complex to analyze, and fluorine functionalization is established by F–Cr and F–C bonds. MXene are also utilized in energy storage, supercapacitors, and sensors applications [44–46].

3.2 Electrochemical study

3.2.1 Biosensor surface engineering

A comprehensive study utilizing both bio-sensing and electrochemical cyclic voltammetry (CV) effectively characterized the sensor's enhancements and modifications, employing the $[Fe(CN)6]^{3-/4-}$ redox probe as a standard electrochemical reference. The CV analysis of the SPCE (Fig. 4, curve a) revealed quasi-reversible behavior, with a significant peak-to-peak separation in the standard solution. Modification with Cr_2C MXene (curve b) resulted in notable cur-

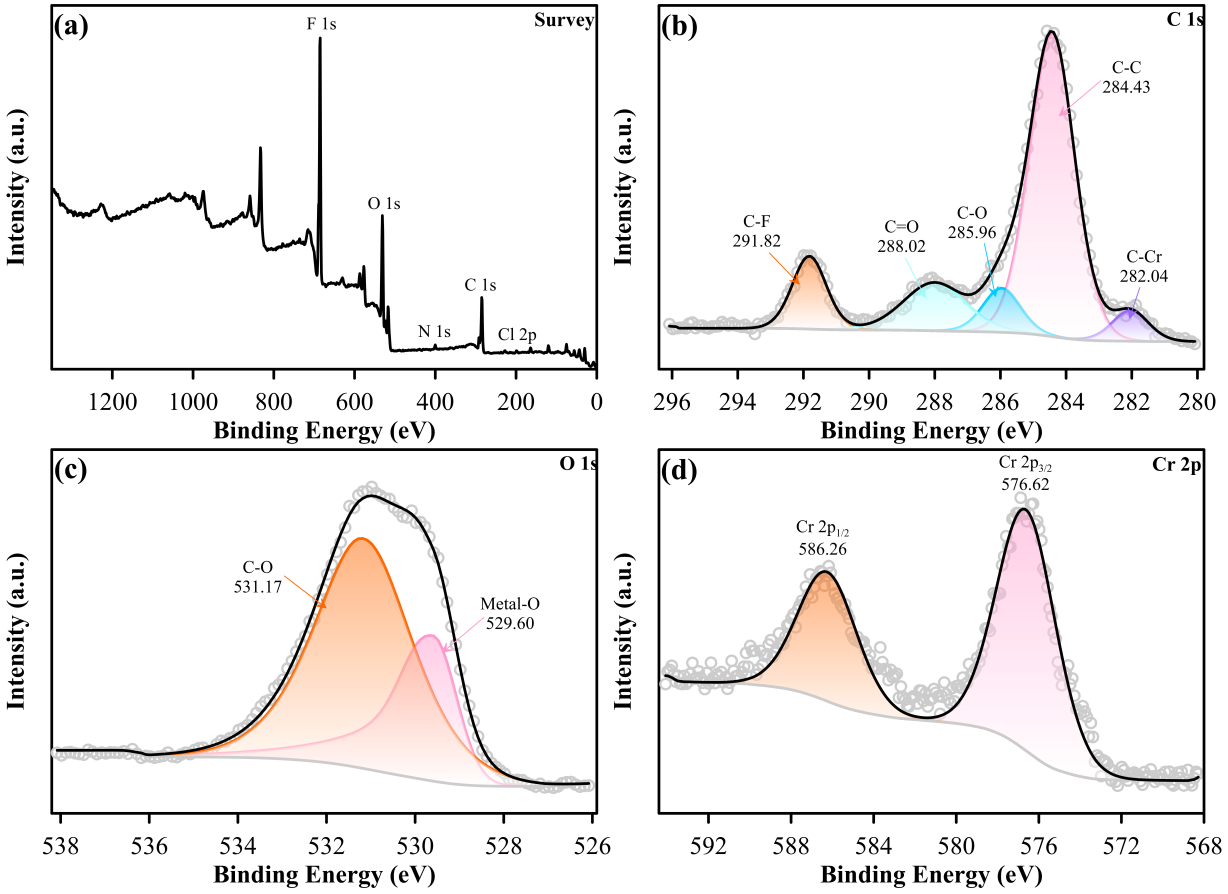

Figure 3. XPS wide range spectra of Cr_2C MAX (a). A survey spectra, C_{1s} (b), O_{1s} (c) and Cr_{2p} (d).

rent enhancements; however, the peak potential remained largely unchanged, representative a lack of catalytic activity. The introduction of AuNPs (curve e) yielded the most significant improvements, leading to reversible behavior for the $[Fe(CN)6]^{3-/4-}$ redox reaction. These findings emphasize the considerable electrochemical influence of both Cr_2C MXene and Au NPs, validating the efficacy of the surface modification strategy.

Upon immobilization of the Pb^{2+}-aptamer onto the Cr_2C MXene/AuNPs composite, a notable reduction in anodic current was observed, representative the formation of an insulating layer on the SPCE/Cr_2CMXene/AuNPs surface. Furthermore, the subsequent introduction of the PSMA protein induced an additional decrease in the anodic signal

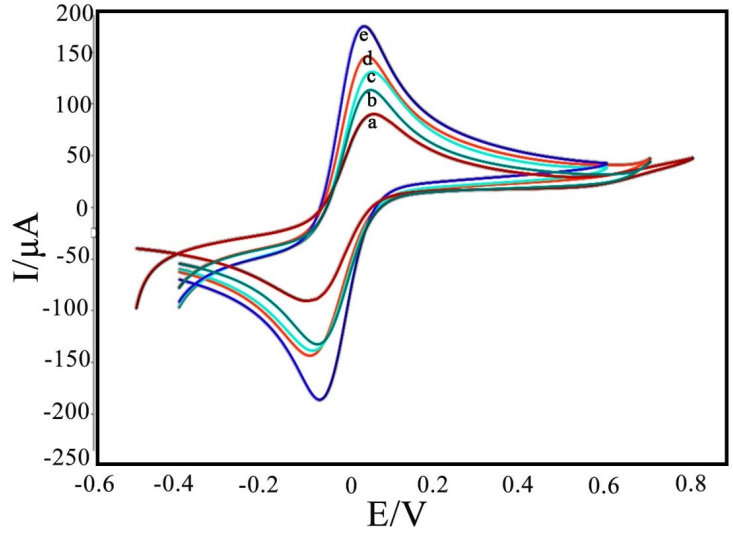

Figure 4. CVs for the following electrode configurations: (a) The bare SPCE, (b) SPCE/Cr_2C MXene, (c) SPCE/Cr_2C MXene/AuNPs/Pb^{2+}-aptamer-PSMA, (d) SPCE/Cr_2C MXene/AuNPs/Pb^{2+}-aptamer, and (e) SPCE/Cr_2C MXene/AuNPs using a 1.0 mM redox probe solution of $[Fe(CN)6]^{3-/4-}$

of the SPCE/Cr_2CMXene/AuNPs/Pb^{2+}-aptamer biosensor, likely due to the inherent low conductivity of the protein. These observations underscore the pivotal role of tailored surface modifications in modulating the electrochemical performance of the developed sensor [47].

3.2.2 Influence of key factors

For boosting the aptasensor's performance, the effect of various concentrations of Pb^{2+} and incubation times was investigated using the PSMA solution (Fig. 5 (A) and 5B). The data indicate that the increase in concentration of Pb^{2+} ($0.5-5$ mM) significantly increased SWASV current, confirming that higher concentrations facilitate the improved adsorption of Pb^{2+} on the aptamer for activity. Beyond the $5-6$ mM range, the signal leveled off, suggesting a maximum response had been attained can be relative saturation of binding sites of aptamer. In terms of time of incubation, increased exposure of PSMA to 90 minutes resulted in a decrease in SWASV current for Pb^{2+}, as PSMA effectively displaced Pb^{2+} from the biosensor matrix. Figure 5 (C) illustrates the impact of different buffer solutions on biosensor efficiency, and Tris-HCl has been better than PBS and Britton-Robinson. Hence, Tris-HCl is the optimal candidate for experimental protocols. This in-depth investigation enables us to identify the predominant parameters that regulate the efficiency of aptasensors and provides a starting point for further optimization.

3.3 Evaluation of the analytical performance of the biosensor

This study wanted to test the ability of SPCE/Cr_2C MXene/AuNPs/Pb^{2+}-aptamer biosensor in detecting the prostate cancer biomarker PSMA under SWASV conditions. The behavior between PSMA and the aptamer was observed by SWASV measurement at the presence and absence of PSMA with concentrations of 100 and 250 pg/mL, as indicated in Fig. 5 (D). A clear-cut decrease in the SWASV peak current was evident upon the introduction of PSMA (curves b and c). It is attributed to the unique interaction between PSMA and the immobilized aptamer on the surface of the SPCE/Cr_2C MXene/AuNPs, resulting in the release of the initially bound Pb^{2+} leads into solution and a concomitant decrease of the SWASV signal (scheme 2).
These results prove the biosensor's capability to detect the PSMA biomarker with success. Additionally, the magnitude of the signal change is directly proportional to PSMA concentration, demonstrating an effective strategy for prostate cancer detection and monitoring. Overall, the SPCE/Cr_2C MXene/AuNPs /Pb^{2+}-aptamer displayed Superior efficiency in monitoring PSMA levels. Figure 6 illustrates that the sensor provided a wide detection window, covering concentrations from 1.0 to 850 pg/mL, with a lin-

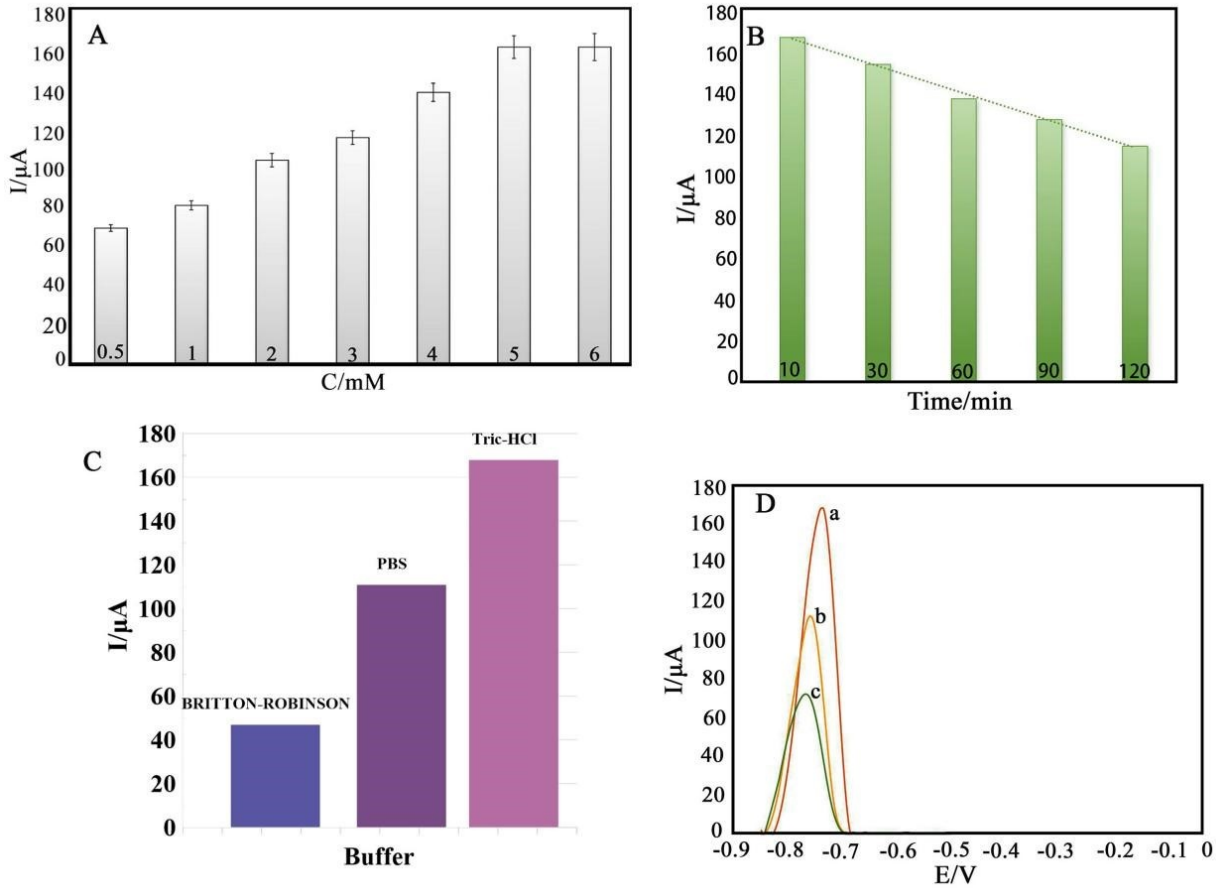

Figure 5. (A) Optimization of Pb^{2+}concentration. (B) Optimization of incubation time with PSMA. (C) Influence of different buffer solutions on the biosensor signal. (D) SWASV illustrating the biosensor response without PSMA (a) and with PSMA at concentrations of 100 pg/mL (b) and 250 pg/mL (c).

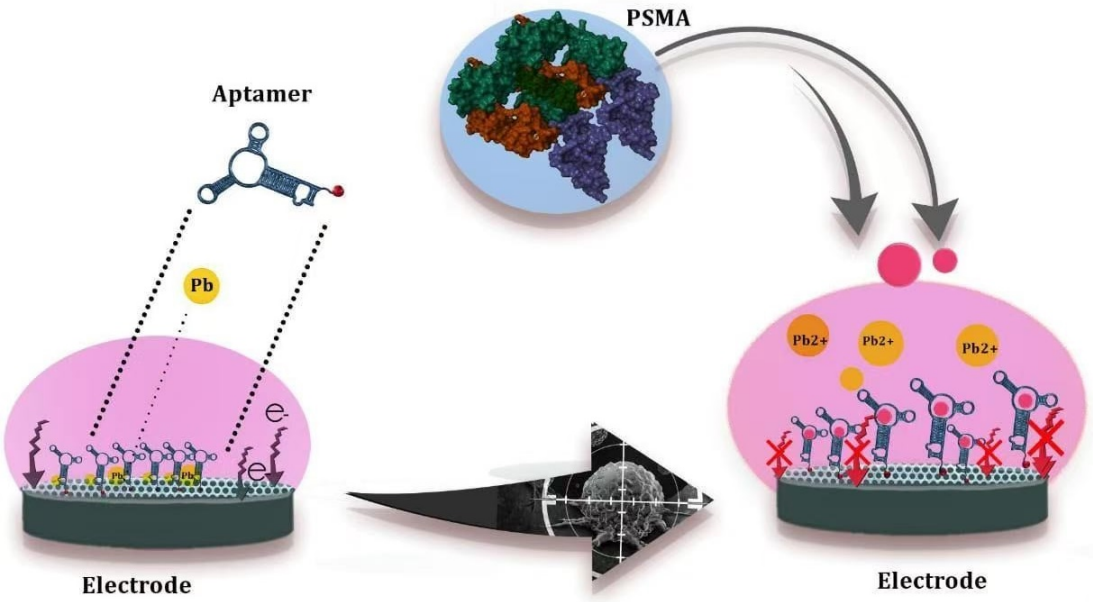

Scheme 2. SPCE/Cr_2C MXene/AuNPs/Pb^{2+}-aptamer biosensor mechanism for diagnosis of PMSA.

ear calibration curve described by $\Delta I = 0.1862\ C + 6.2936$ ($R^2 = 0.9923$).

Shown in the inset are the SWASV curves for PSMA solutions spanning $1.0 - 850$ pg/mL (a–j) recorded on the SPCE/Cr_2C MXene/AuNPs/Pb^{2+}-aptamer interface. The sensor reached a remarkably low LOD of 3.22 fg/mL, outperforming previously published designs (Table 1). The reported LOD, significantly lower than the 9.5 ng/mL of carbon fiber modified sensor and 48.2 ng/mL of Cys-AuNP/SPGE reported in Table 1. Its dynamic range of $1.0 - 850$ pg/mL also exceeds that of other modifications, such as Fe_3O_4@SiO_2@6Pha nanoparticles. Additionally, the enhanced stability from this design addresses common performance issues in existing biosensors. Overall, this work demonstrates considerable advancements in sensitivity, range, and reliability.

The biosensor exhibited a good level of selectivity for 400 pg/mL PSMA monitoring, as shown in Fig. 7 (a). In terms of stability, the biosensor's response to PSMA was evaluated over several weeks. As illustrated in Fig. 7 (b), it demonstrated strong performance during the initial three weeks for detects 300 pg/mL PSMA. However, a decline in detection capability was observed thereafter. It was observed that the biosensor remained stable and dependable in detecting PSMA for a period of roughly 21 days; however, its quantitative capability began to weaken thereafter.

In this final step, the application of SPCE/Cr_2C MXene/AuNPs/Pb^{2+}-AP as a new biosensor for the detection of PSMA

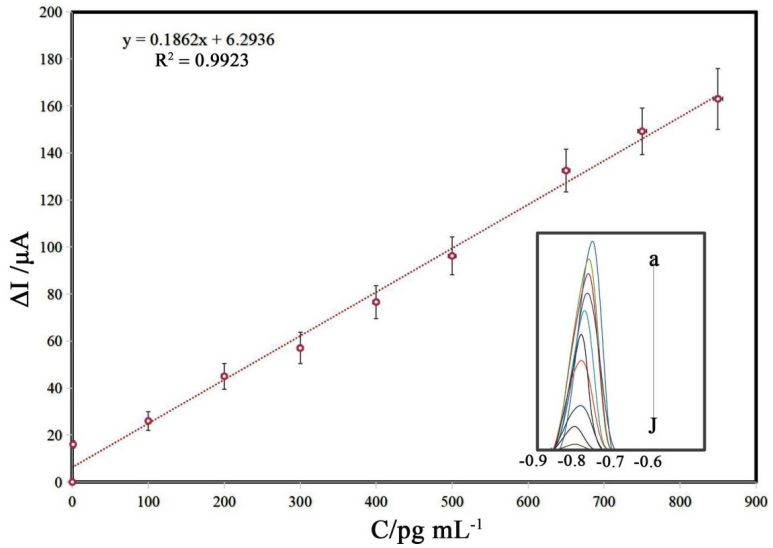

Figure 6. Presents the calibration curve for the incubated aptasensor subjected to different concentrations of PSMA. The inset provides a detailed view of the SWASV signals corresponding to PSMA solutions within the range of 1.0 to 850 pg/mL (a–J) at the SPCE/Cr_2C MXene/Au NPs/Pb^{2+}-aptamer interface (n = 4).

Table 1. Evaluation of the Performance of the developed electrochemical aptasensor for PSMA diagnosis.

Electrode	Modifier	LDR	LOD	Ref.
Carbon	Carbon fiber	10 – 200 ng/mL	9.5 ng/mL	[48]
SPGE	Cys-AuNP/SPGE	5 – 250 ng/mL	48.2 ng/mL	[49]
	Fe_3O_4@SiO_2@6Pha nanoparticles	7.5 – 1250 pg/mL	2.21 pg/mL	[50]
SPCE	SPCE/Cr_2C MXene/AuNPs/Pb^{2+}-AP	1 – 850 pg/mL	3.22 fg/mL	This work

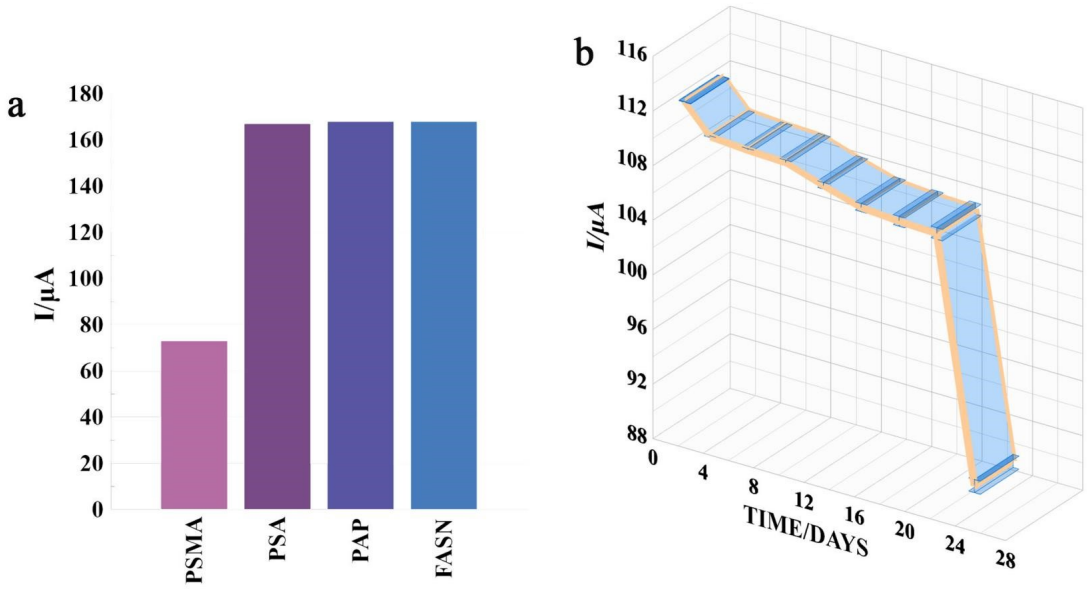

Figure 7. (a) Evaluation of the specificity of the PSMA aptasensor. (b) Long-term stability test of the aptasensor in PSMA detection over a 24-day period.

in dextrose saline as a real matrix was evaluated. Using the standard addition method, a recovery range between 96.7% and 102.1% was detected for the monitoring of PSMA by SPCE/Cr_2C MXene/AuNPs/Pb^{2+}-AP, which is an acceptable range for a new biosensor.

4. Conclusion

This work is a novel biosensor developed for accurate detection and monitoring of the PSMA prostate cancer biomarker. It employs an advanced layering approach, where a Cr_2C MXene/AuNPs/Pb^{2+}-AP layer acts as the SPCE modifier. The aptasensor architecture leverages MXene, gold nanoparticles, and a PSMA-specific aptamer to boost sensitivity and facilitate point-of-care detection of PSMA. Selective investigations of the SPCE/Cr_2C MXene/AuNPs/Pb^{2+}-AP sensor successfully differentiate PSMA from other prostate biomarkers. The biosensor is designed to detect PSMA by utilizing Pb^{2+} as a signaling molecule to analyze PSMA concentrations. It can accurately measure PSMA levels ranging from 1.0 to 850 pg/mL, boasting an exceptional LOD of 3.22 fg/mL. Interestingly, the biosensor is highly selective for PSMA despite the presence of other prostate cancer biomarkers such as prostate-specific antigen (PSA), prostatic acid phosphatase (PAP), and fatty acid synthase (FASN). Utilization of this technology involves overcoming nanomaterial optimization, toxicity of Pb^{2+}, fouling of the electrode, and sustaining reproducibility. This confirms that the biosensor possesses the potential to significantly reduce the reliance on invasive therapy in the treatment of prostate cancer.

Authors Contribution
All authors assisted to the conceptualization, literature review, experimental work, data sample analysis, as well as writing, formatting, and editing of the manuscript.

Availability of data and materials
The data that support the findings of this study are available from the corresponding author, upon reasonable request.

Conflict of interests
The authors declare that they have no known competing financial interests or personal relationships that could have appeared to influence the work reported in this paper.

References

[1] G.B.D.C. Collaboration. "Global, regional, and national cancer incidence, mortality, years of life lost, years lived with disability, and disability-adjusted life-years for 29 cancer groups, 1990 to 2017: A systematic analysis for the global burden of disease study". *JAMA Oncol*, **5**(1749-1768), 2019.

[2] B. Singh, S. Ma, T.O. Hara, et al. "Nanomaterials-based biosensors for the detection of prostate cancer biomarkers: recent trends and future perspective". *Adv Mater Technol*, **8**(2201860), 2023.

[3] F. Obafemi and G. Umahi-Ottah. "A review of global Cancer prevalence and therapy". *J Cancer Res Treat Prev*, **1**:128–147, 2023.

[4] E.D. Crawford. "Epidemiology of prostate cancer". *Urology*, **62**: 3–12, 2003.

[5] J. Cuzick, M.A. Thorat, G. Andriole, et al. "Prevention and early detection of prostate cancer". *Lancet Oncol*, **15**:e484–e492, 2014.

[6] J. Li, W. Cheng, C. Wang, et al. "Peptide-based electrochemical detection of prostate cancer-derived exosomes using a dual signal amplification strategy". *Sens Actuators Rep*, **7**:100202, 2024.

[7] K. Permpoka, P. Kaewarsa, W. Paekoh, et al. "A Capacitance Biosensor for Prostate Cancer Detection via Normalised Urinary Extracellular Vesicles". *Biosens Bioelectron*, **288**:117791, 2025.

[8] L. Yan, Y. Zhang, Q. Guo, et al. "Autoluminescent Met-AuNCs mediated coreactant-free electrochemiluminescent biosensor based on DNA walker cascade signal amplification for Vibrio parahaemolyticus detection". *Sens Actuators B*, **408**:135536, 2024.

[9] X. Wang, X. Hu, S. Pan, et al. "DNA and ATP synergistically triggered Argonaute-mediated sensor for the ultrasensitive detection of viable Salmonella without DNA extraction and amplification". *Sens Actuators B*, **408**:135543, 2024.

[10] R. Mayeux. "Biomarkers: Potential uses and limitations". *NeuroRx*, **1**:182–188, 2004.

[11] K. Strimbu and J.A. Tavel. "What are biomarkers?". *Current Opinion in H&A*, **5**:463–466, 2010.

[12] R.M. Califf. "Biomarker definitions and their applications". *Exp Biol Med*, **243**:213–221, 2018.

[13] M. Eder, M. Eisenhut, J. Babich, et al. "PSMA as a target for radiolabelled small molecules". Springer:819–823, 2013.

[14] N. Woythal, R. Arsenic, C. Kempkensteffen, et al. "Immunohistochemical validation of PSMA expression measured by 68Ga-PSMA PET/CT in primary prostate cancer". *J Nucl Med*, **59**:238–243, 2018.

[15] R. Alipour, A. Azad, and M.S. Hofman. "Guiding management of therapy in prostate cancer: Time to switch from conventional imaging to PSMA PET?". *Ther Adv Med Oncol*, **11**:1758835919876828, 2019.

[16] A.M. Chiorcea-Paquim. "Advances in electrochemical biosensor technologies for the detection of nucleic acid breast cancer biomarkers". *Sensors*, **23**:4128, 2023.

[17] C. Zhu, G. Yang, H. Li, et al. "Electrochemical sensors and biosensors based on nanomaterials and nanostructures". *Anal Chem*, **87**: 230–249, 2015.

[18] M. Gandhi, J. Indiramma, N.S. Jayaprakash, et al. "An efficient electrochemical sandwich ELISA for urinary human serum albumin-biomarker based on highly redox-active thionine surface-confined MWCNT/PEDOT PSS platform". *J Electroanal Chem*, **906**:116018, 2022.

[19] S. Cheraghi, M.A. Dasar, and M.A. Taher. "Fe_3O_4/RGO-Ionic liquid Nanocatalyst as Amplifier for Fabrication of Highly Sensitive Electrochemical Sensor in Monitoring of Thallium Environmental Fluids". *J Nanostructure Chem*, **15**:152510, 2025.

[20] S. Afzal, A. ur Rehman, T. Najam, et al. "Recent advances of MXene@ MOF composites for catalytic water splitting and wastewater treatment approaches". *Chemosphere*, **364**:143194, 2024.

[21] X. Qiu, Y. Zheng, H. Li, et al. "Unveiling gas transport mechanisms in tunable MXene nanochannels: Insights from molecular dynamics simulations". *J Membr Sci*, **715**:123459, 2025.

[22] K.R.G. Lim, M. Shekhirev, B.C. Wyatt, et al. "Fundamentals of MXene synthesis". *Nat. Synth.*, **1**:601–614, 2022.

[23] J. Sun, B. Liu, Q. Zhao, et al. "MAX, MXene, or MX: What are they and which one is better?". *Adv Mater*, **35**:2306072, 2023.

[24] A. Thakur, N. Chandran, K. Davidson, et al. "Step-by-step guide for synthesis and delamination of $Ti_3C_2T_x$ MXene". *Small Methods*, **7**: 2300030, 2023.

[25] M. Downes, C.E. Shuck, B. McBride, et al. "Comprehensive synthesis of $Ti_3C_2T_x$ from MAX phase to MXene". *Nat Protoc*, **19**: 1807–1834, 2024.

[26] A.H. Arshad, S. Riaz, M.D. Hussain, et al. "MXene and MXene-based hybrid materials for pharmaceutical-induced pollutants removal via adsorption and photocatalysis: A critical viewpoint". *Environ Technol Rev*, **14**:142–190, 2025.

[27] S. Bibi, S.S.A. Shah, M.A. Nazir, et al. "MOF/MXene composites: Synthesis, application and future perspectives". *Adv Sustain Syst*, **8**: 2400011, 2024.

[28] M.A. Nazir, T. Najam, S. Ullah, et al. "Recent advances in MXene nanomaterials: Fundamentals to applications in environment sector". *EcoEnergy*, **2**:505–548, 2024.

[29] T. Wu, Y. Li, Z. Zhang, et al. "3D Print-Based Polypyrrole/TiVCT$_x$/UiO-66 Composites for Effective Adsorption of Combined Pollutants in Water Media". *J Nanostructure Chem*, **15**:152503, 2025.

[30] C. Liang, J. He, Y. Cao, et al. "Advances in the application of Mxene nanoparticles in wound healing". *J Biol Eng*, **17**:39, 2023.

[31] N. Baig, I. Kammakakam, and W. Falath. "Nanomaterials: A review of synthesis methods, properties, recent progress, and challenges". *Mater Adv*, **2**:1821–1871, 2021.

[32] X. Wu, P. Ma, Y. Sun, et al. "Application of MXene in electrochemical sensors: A review". *Electroanalysis*, **33**:1827–1851, 2021.

[33] L. Jia, Z. Lei, N. Zare, et al. "Ti_3C_2 MXene-enhanced Electrochemical Biosensors for Prostate-Specific Antigen (PSA) Detection in Prostate Cancer". *J Nanostructure Chem*, **15**:152502, 2025.

[34] X. Bai and J. Guan. "Applications of MXene-based single-atom catalysts". *Small Struct*, **4**:2200354, 2023.

[35] C. Zhou, X. Zhao, Y. Xiong, et al. "A review of etching methods of MXene and applications of MXene conductive hydrogels". *Eur Polym J*, **167**:111063, 2022.

[36] H. Ahmad, K. Kamaruzzaman, M.Z. Samion, et al. "MXene-Cr_2C as a novel saturable absorber for mode-locking at 2.07 μm". *Opt Mater*, **160**:116713, 2025.

[37] G. Fagerlund. "Determination of specific surface by the BET method". *Mater Struct*, **6**:239–245, 1973.

[38] K.S. Walton and R.Q. Snurr. "Applicability of the BET method for determining surface areas of microporous metal-organic frameworks". *JACS*, **129**:8552–8556, 2007.

[39] M. Alimohamadi, A. Khataee, S. Arefi-Oskoui, et al. "Catalytic activation of hydrogen peroxide by Cr_2AlC MAX phase under ultrasound waves for a treatment of water contaminated with organic pollutants". *Ultrason Sonochem*, **93**:106294, 2023.

[40] X. Zou, H. Liu, H. Xu, et al. "A simple approach to synthesis Cr_2CT_x MXene for efficient hydrogen evolution reaction". *Mater Today Energy*, **20**:100668, 2021.

[41] N. Trainor. "Survey of Etching Techniques to Produce Cr_2C MXene from Cr_2AlC, Drexel University". 2019.

[42] L. Guo, H. Han, J. Wang, et al. "Defective Cr_2CT_x-based sensors with high sensitivity for NO_2 detection at room temperature". *J Mater Chem A*, **12**:20414–20424, 2024.

[43] F. Zažímal, D. Plašienka, and S. Atri. "Unveiling the effect of the polymerization degree of graphitic carbon nitride on the surface functionalization by low-temperature plasma: Insights from XPS and DFT study". *Appl Surf Sci*, **699**:163073, 2025.

[44] R. Darabi and M. Shabani-Nooshabadi. "ZIF-8/Co-C3N4-GNR/MXene nanocomposites: A novel electrode material with excellent electrochemical properties for supercapacitors". *Alex Eng J*, **129**:803–810, 2025.

[45] X. Kong, C. Fan, K. Liao, et al. "MXenes for wearable pressure sensing: Progress and prospects in human motion detection". *Alex Eng J*, **118**:466–481, 2025.

[46] F. Abbasi, F. Boorboor Ajdari, M. Mansournia, et al. "Toward high energy and durable anodes: Critical review on $Li_4Ti_5O_{12}$–MXene composites". *Carbon Lett*, **35**:515–537, 2025.

[47] N. Zare, H. Karimi-Maleh, Z. Zhang, et al. "Enhancing cancer biomarker identification: Precise monitoring of MUC1 using V_2C/Au nanocomposite-amplified electrochemical biosensor". *Carbon Lett*, **35**:1691–1700, 2025.

[48] Z. Rezaei, I. Alemzadeh, and M. Vossoughi. "Design and fabrication of an electrochemical-based nanofibrous immunosensor for detection of prostate cancer biomarker, PSMA". *Polym Adv Technol*, **33**:1967–1977, 2022.

[49] G. Kabay, Y. Yin, C.K. Singh, et al. "Disposable electrochemical immunosensor for prostate cancer detection". *Sens Actuators B*, **360**:131667, 2025.

[50] M. Aydın, E.B. Aydın, and M.K. Sezgintürk. "Functionalized magnetic nanoparticles for electrochemical magneto biosensing of PSMA cancer biomarker". *New J Chem*, **48**:5769–5781, 2024.